

9-24-1996

## Fluorescence Imaging and Spectroscopy of Biomaterials in Air and Liquid by Scanning Near-Field Optical/Atomic Force Microscopy

H. Muramatsu

*Seiko Instruments Inc.*, [muramatu@tk.sii.co.jp](mailto:muramatu@tk.sii.co.jp)

N. Chiba

*Seiko Instruments Inc.*

K. Nakajima

*Seiko Instruments Inc.*

T. Ataka

*Seiko Instruments Inc.*

M. Fujihira

*Tokyo Institute of Technology*

Follow this and additional works at: <https://digitalcommons.usu.edu/microscopy>



Part of the [Biology Commons](#)

---

### Recommended Citation

Muramatsu, H.; Chiba, N.; Nakajima, K.; Ataka, T.; Fujihira, M.; Hitomi, J.; and Ushiki, T. (1996)  
"Fluorescence Imaging and Spectroscopy of Biomaterials in Air and Liquid by Scanning Near-Field  
Optical/Atomic Force Microscopy," *Scanning Microscopy*: Vol. 10 : No. 4 , Article 6.  
Available at: <https://digitalcommons.usu.edu/microscopy/vol10/iss4/6>

This Article is brought to you for free and open access by  
the Western Dairy Center at DigitalCommons@USU. It  
has been accepted for inclusion in Scanning Microscopy  
by an authorized administrator of DigitalCommons@USU.  
For more information, please contact  
[digitalcommons@usu.edu](mailto:digitalcommons@usu.edu).



---

# Fluorescence Imaging and Spectroscopy of Biomaterials in Air and Liquid by Scanning Near-Field Optical/Atomic Force Microscopy

## Authors

H. Muramatsu, N. Chiba, K. Nakajima, T. Ataka, M. Fujihira, J. Hitomi, and T. Ushiki

## FLUORESCENCE IMAGING AND SPECTROSCOPY OF BIOMATERIALS IN AIR AND LIQUID BY SCANNING NEAR-FIELD OPTICAL/ATOMIC FORCE MICROSCOPY

H. Muramatsu\*, N. Chiba, K. Nakajima, T. Ataka, M. Fujihira<sup>1</sup>, J. Hitomi and T. Ushiki<sup>2</sup>

Research Lab. for Advanced Tech., Seiko Instruments Inc., Takatsuka-shinden, Matsudo-shi, Chiba 271, Japan

<sup>1</sup>Dept. of Biomolecular Engineering, Tokyo Institute of Technology, Nagatsuta, Midori-ku, Yokohama 227, Japan

<sup>2</sup>Dept. of Anatomy and Histology, Niigata University School of Medicine, Asahimachi-dori 1, Niigata 951, Japan

(Received for publication April 1, 1996 and in revised form September 24, 1996)

### Abstract

We have developed scanning near-field optical/atomic force microscopy (SNOM/AFM). The SNOM/AFM uses a bent optical fiber simultaneously as a dynamic force AFM cantilever and a SNOM probe. Resonant frequency of the optical fiber cantilever is 15-40 kHz. Optical resolution of the SNOM/AFM images shows less than 50 nm. The SNOM/AFM system contains photon counting system and polychromator/intensified coupled charge device (ICCD) system to observe fluorescence image and spectrograph of micro areas, respectively. Cultured cells were stained with fluorescein isothiocyanate (FITC)-labeled anti-keratin antibody or FITC-labeled phalloidin after treatment with Triton X-100. Fluorescence and topographic images were obtained in air and water. The fluorescence images showed clear images of keratin and actin filaments. The SNOM/AFM is perfect to observe biomaterials in liquid with a liquid chamber while the topographic images showed subcellular structures which correspond to keratin and actin filaments.

**Key Words:** Actin filaments, atomic force microscopy, biomaterials, chromium, fluorescence imaging, keratin filaments, scanning near-field optical microscopy.

### Introduction

Scanning near-field optical/atomic force microscopy (SNOM/AFM) is an excellent tool to observe biological materials because it provides simultaneously topographic and optical images in high resolution. The resolution of topographic and optical images is much higher than that of the conventional far-field microscopy. Unlike electron microscopy, SNOM/AFM can observe samples in air and liquid. SNOM/AFM has also advantage to give various information such as fluorescence images and spectrographs in a micro area [7].

Various kinds of scanning near-field optical microscopy have developed in the variation of method to control tip-sample separation such as utilizing scanning transmission microscopy (STM) [5], lateral shear force [1], and contact-mode AFM [13, 15]. Aaron Lewis and coworkers originally developed SNOM/AFM using bent capillary tubes in which fluorescence material is settled on the tip of the tube to illuminate a sample surface [13]. After that, we developed the bent optical wave guide probe for the current type SNOM/AFM in which a method of the dynamic mode AFM was used to control the tip-sample separation [2, 9]. An optical fiber with a sharpened tip was bent for using the probe as a cantilever for AFM, and the vibration amplitude of the cantilever was held constant during scanning. The SNOM/AFM may be superior in biological observation to other SNOM systems because this system operates excellently in liquids [10]. It is safely applicable for observation of soft samples with great variations in height, such as cultured cells. The SNOM/AFM may also be superior in liquid to other cyclic contact AFM (e.g., tapping mode); the latter use flat type cantilevers [4, 6, 12], while the optical-fiber cantilever of SNOM/AFM is round, which helps to reduce viscositic resistance of liquid. In the case of the shear force mode, AFM may work in liquid but, to our knowledge, there are no published images of biological materials in liquid, such as cultured cells. In the tuning fork mode, where a tuning fork is used for the force detection of an optical fiber glued onto the fork [8], AFM needed improvement

\*Address for correspondence:

Hiroshi Muramatsu

Research Laboratory for Advanced Technology,

Seiko Instruments, Inc.,

Takatsuka-shinden, Matsudo-shi,

Chiba 271, Japan

Telephone number: 81-473-92-7880

FAX number: 81-473-92-7822

E-mail: muramatu@tk.sii.co.jp

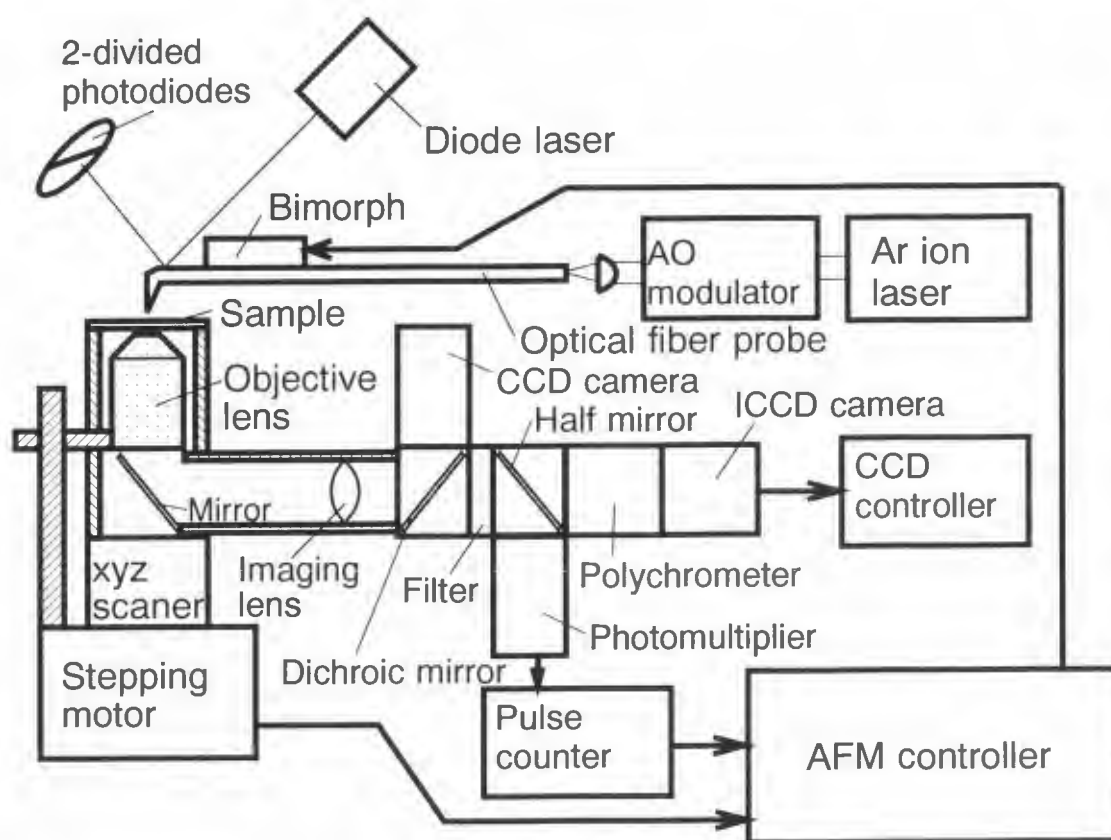


Figure 1. Schematic diagram of SNOM/AFM system.

for use in liquid because electrodes are patterned on the surface of the tuning fork, and electrical leakage would inhibit function in aqueous solution.

This paper reports the performance of SNOM/AFM in the observation of a standard specimen of chromium patterns and fluorescence beads and displays fluorescence SNOM/AFM images of cultured cells in the air and an aqueous solution.

### Experimental Setup

The SNOM/AFM system is shown in Figure 1. The optical-fiber cantilever is mounted on a bimorph and vibrated vertically against the specimen stage at the resonant frequency (typically 15–40 kHz). The vibration voltage applied on the bimorph was between 0.1 and 5 ACV<sub>p-p</sub> for 0.11 nm/V bimorph. The vibration amplitude is monitored by detecting the deflection of the laser beam, which is reflected on the ground surface of the optical fiber cantilever. The probe tip-sample distance is controlled by decreasing the vibration amplitude to a appropriate level when the distance between the probe tip and the sample decrease. This operation was con-

trolled by a commercialized AFM controller (model SPI 3700, Seiko Instruments, Chiba, Japan).

Laser beams of multi-line Ar ion laser (maximum 150 mW) were selected by polychromatic acoustic optical (AO) modulator and coupled to the optical fiber on the other side of optical fiber probe. Signal light from the sample is collected by objective lens (typically: 100 X oil immersion type) and separated by dichroic mirror to the coupled charge devise (CCD) camera and detectors. Photomultiplier and intensified-CCD camera with spectrometer are connected as the detectors.

Figure 2 shows a liquid chamber designed for the present experiment. Water and cell culture media were held between the glass plate and an upper window. Both the probe and the sample were immersed in solution.

The probe was prepared as previously described [2]. Briefly, an optical fiber, single mode for wavelength of 500 nm, was sharpened by chemical etching to make a tip, and then bent with irradiation of a CO<sub>2</sub> laser. The chemical etching is performed at room temperature for 45 minutes in 50% HF solution. CO<sub>2</sub> laser is at a maximum of 25 W and modulated to control power. Un-focused laser beam is used for bending. The probe was



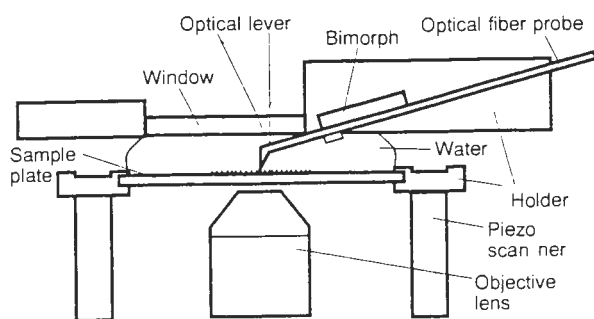


**Figure 2.** Schematic diagram of the liquid chamber in SNOM/AFM system.

coated with a 100-200 nm-thick metal layer (aluminum or gold), and an aperture was made by vapor deposition in rotating optical fiber tip (Fig. 3).

The spring constant was approximated by a spring constant equation for a rod:

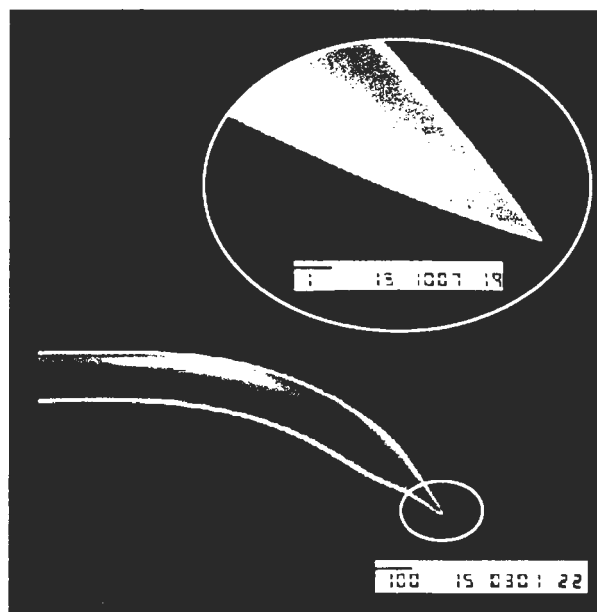
$$k = \frac{3\pi d^4 E}{64l^3} \quad (1)$$

where  $k$  is the spring constant,  $d$  is the diameter of the rod,  $E$  is Young's modulus, and  $l$  is the length of the rod. A spring constant for 3 mm long probe was calculated at 97 N/m.  $Q$  factor is typically 200-600 in the air and 20-200 in water [11]. The oscillation amplitude employed was between 10-100 nm (0.1-1 ACV<sub>p-p</sub> in the air, or 0.5-5 ACV<sub>p-p</sub> in water for driving the bimorph). Under typical imaging conditions, average sample-probe separation was controlled by the amplitude of the vibration, which became 80-96% of the free vibration amplitude. The interaction force between the probe and the sample was as small as that of normal cyclic contact mode AFM.

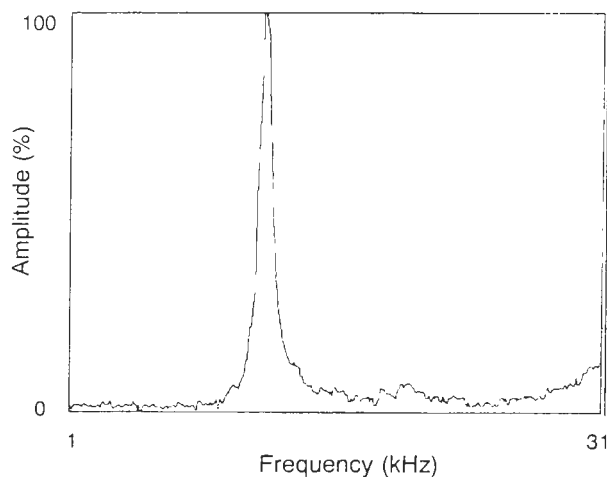
The advantage of the instrument operating in liquid was proved by resonance curves of an optical fiber probe and a silicon cantilever in liquid. The resonance curve for the silicon cantilever showed many peaks and was not stable, but that for the optical fiber probe showed a clear single resonance peak in liquid, as seen in Figure 4.

## Results and Discussion

Figures 5a and 5b show representative topographic and optical images of a standard sample observed with a 514.5 nm laser beam. The standard sample is a patterned chromium layer of 2  $\mu\text{m}$  by 2  $\mu\text{m}$  checker with 20 nm thickness on a quartz glass plate. In the topographic image, the higher part shows the chromium

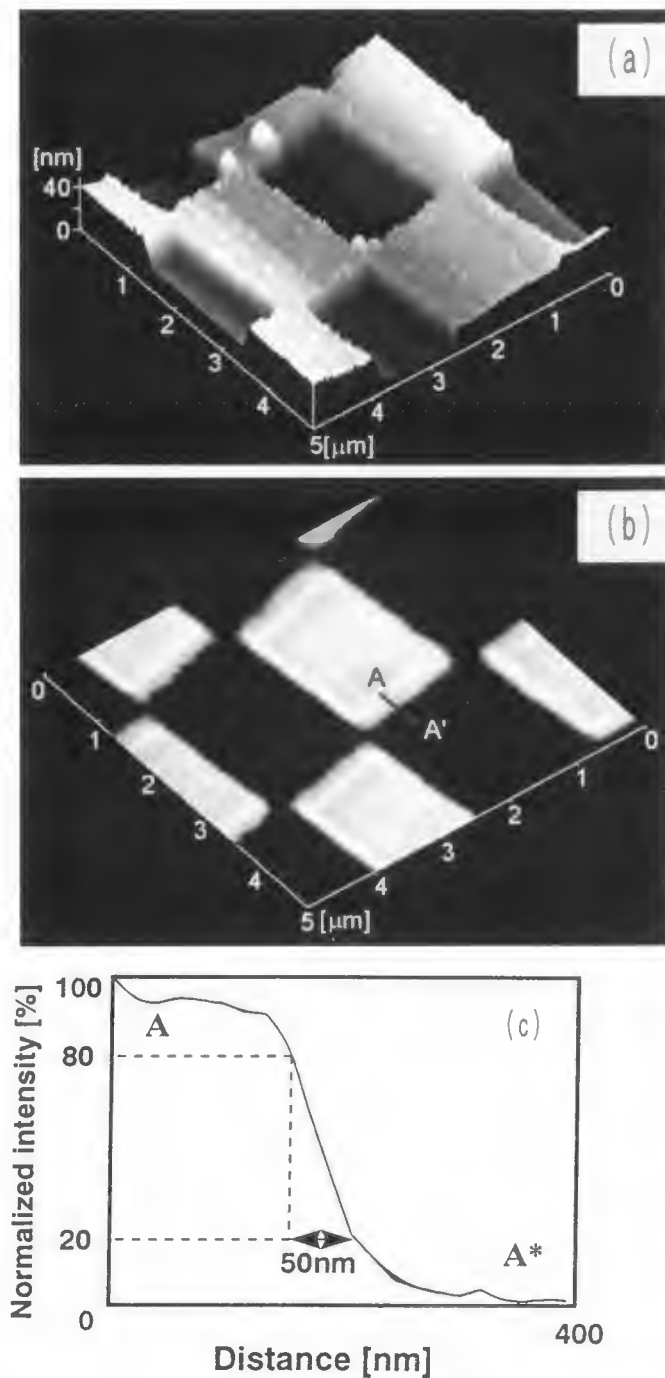


**Figure 3.** A representative scanning electron microscope image of the probe made from an optical fiber coated with aluminum.



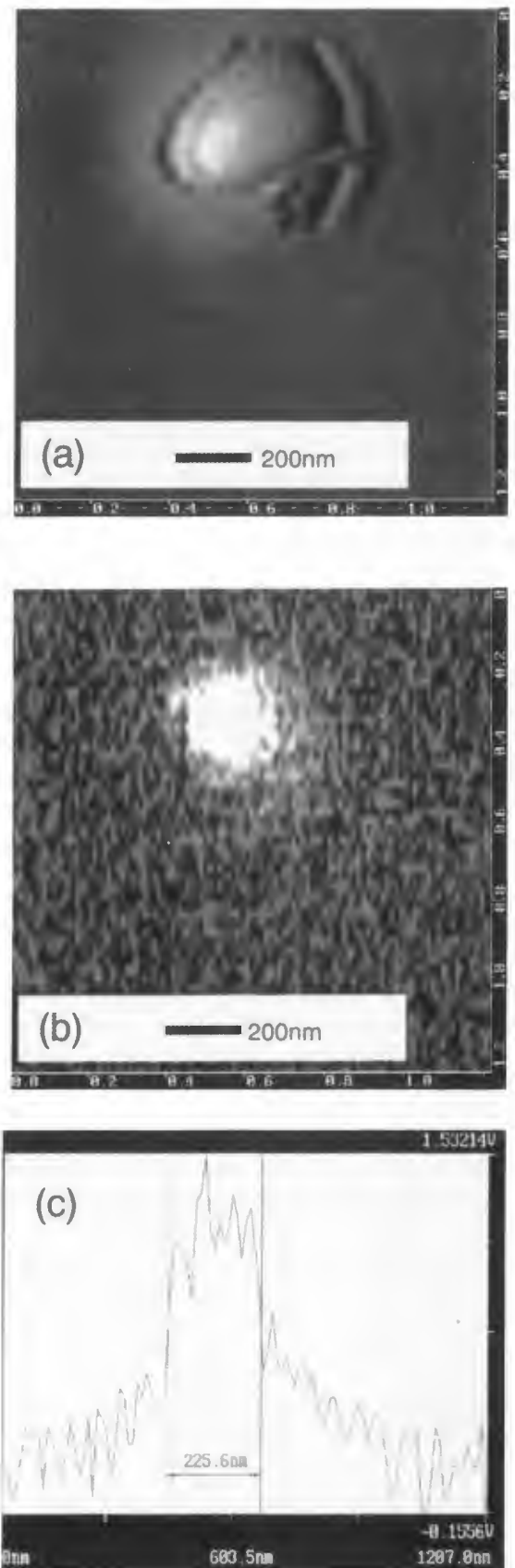
**Figure 4.** Typical resonance curve for the optical fiber cantilever in water. The resonant frequency is 12.2 kHz, and the  $Q$  factor is 23.

layer. The chromium layer produces dark parts in the optical image because the chromium layer blocks the transmitting a light from the optical fiber probe to the objective lens. In the SNOM/AFM operation, the laser beam was modulated with an AO modulator by the same frequency of probe vibration. The phase between probe vibration and irradiation cycle was tuned as the irradiation allows when the tip-sample separation is smallest in



**Figure 5.** Topographic (a) and near-field optical (b) images of a standard chromium pattern on quartz glass plate. The optical profile (c) of A-A' in Figure 5b. A\* of Figure 5c is equivalent to the A' of Figure 5b.

**Figure 6 (at right).** Topographic (a) and fluorescence (b) images of 100 nm fluorescence beads coated with PVA film on a cover glass. The fluorescence profile (c) of fluorescence of the beads in Figure 6b. Scan area is  $1.2 \mu\text{m}$  by  $1.2 \mu\text{m}$ .



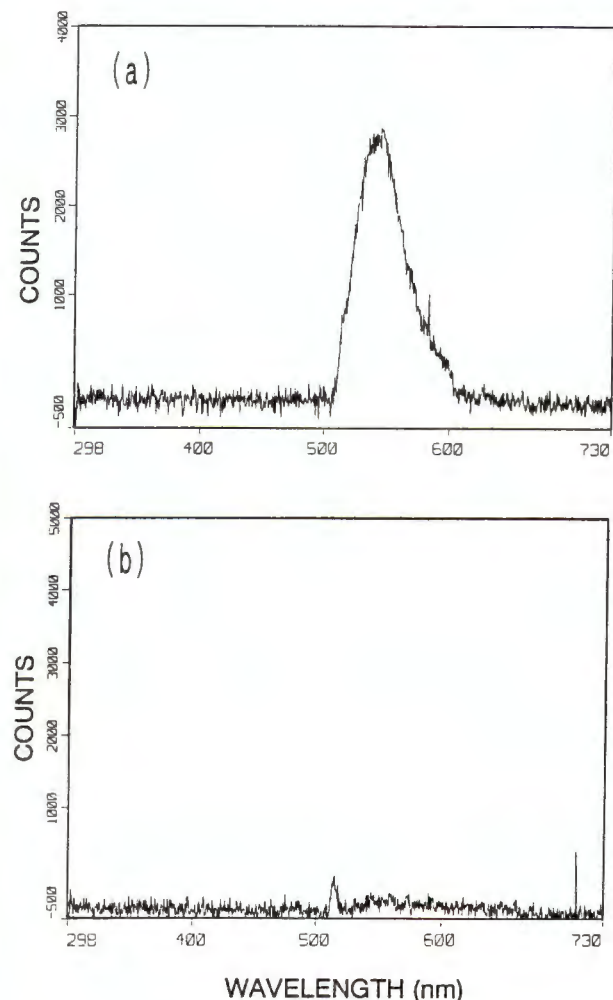


**Figure 7.** Spectrograph with 488 nm excitation when the probe tip was on the fluorescence beads (a) and 750 nm from the beads (b).

the vibration cycle. The separation between the tip and sample surface is a factor in the resolution of the optical image; for example, illuminating in wide separation decreases the optical resolution. When illumination is performed at the range of smallest separation during the vibration, the resolution will be kept in high level [3].

Figure 5c shows the optical profile which is marked as A-A' in Figure 5b. Generally, the resolution is defined as a distance of two particles or point-light-sources which can be imaged separately. In the case of point-light-sources, the distance of the two points should be slightly wider than the width of the half peak value (50%) of the gaussian profile which was detected by the probe. A width of 40% of the peak value enables a tip to image the two points separately. We applied this concept to the step of the metal layer. If the probe scans on a pin hole which is smaller than the aperture, the profile

of optical image will be a reflected image of optical profile at intensity between 0% to 50%. The width of 20 to 80% in Figure 5c corresponds to the width of 40% of the left slope and 40% of the right slope of the peak in the reflected image. Actually, the width of the slope between the dark part and bright part shows 50 nm in 20-80% threshold.

When the probe tip is just on the edge of the chromium step, a half of the aperture is on the chromium layer while the other half of the aperture is 20 nm above the glass surface. This 20 nm distance is significant, particularly when considering the spreading of light at a coupling region of near field wave. Therefore, the aperture of the probe must be smaller than the width of slope, i.e., the aperture is smaller than 50 nm in this result.

In the fluorescence measurement, we used the photon counting type photomultiplier instead of the analog type photomultiplier in the transmission mode. Topographic and fluorescence images of 100 nm fluorescence beads are shown in Figures 6a and 6b, where beads were spread on cover glass with poly-vinyl-alcohol (PVA) film by spin coating the beads and PVA solution mixture to control the density of the beads on the glass plate. The PVA film was prepared thinner than the height of beads to enable the tip imaging topography and optical image of beads. The topographic image shows a round shape of beads and wrinkles of PVA film around the beads. The fluorescence image was observed with a 488 nm laser beam for excitation and showed the clear round shape of the fluorescence beads. The profile of fluorescence intensity of Figure 6b shows that the width of the fluorescence peak for the beads is about 200 nm (Fig. 6c). In this case, the diameter of the beads is 100 nm. In the fluorescent beads experiment, we used a probe which showed 100 nm resolution of our step sample, therefore, this result is reasonable. Scattering light produced at probe tip and sample surface may cause the slope of the fluorescence profile of the beads extending about 500 nm to the right and to the left of the peak. The slope profile may depend on the structural factor of the probe and sample surface.

Figure 7a is a fluorescence spectrograph, taken when the probe tip was on the fluorescence beads. In this experiment, the spectrum window is limited to a 515 to 600 nm range, because the system has a dichroic mirror of 500 nm and long wave pass filter of 515 nm to cut the excitation light, and short wave pass filter of 600 nm to cut the laser beam of optical lever (670 nm). The long wave pass filter will be removed when a self-sensitive probe, such as the tuning fork probe, is used. When the probe tip was located at 750 nm of lateral movement from the center of the beads, the spectrograph showed only a small peak of 514.5 nm (Fig. 7b). This



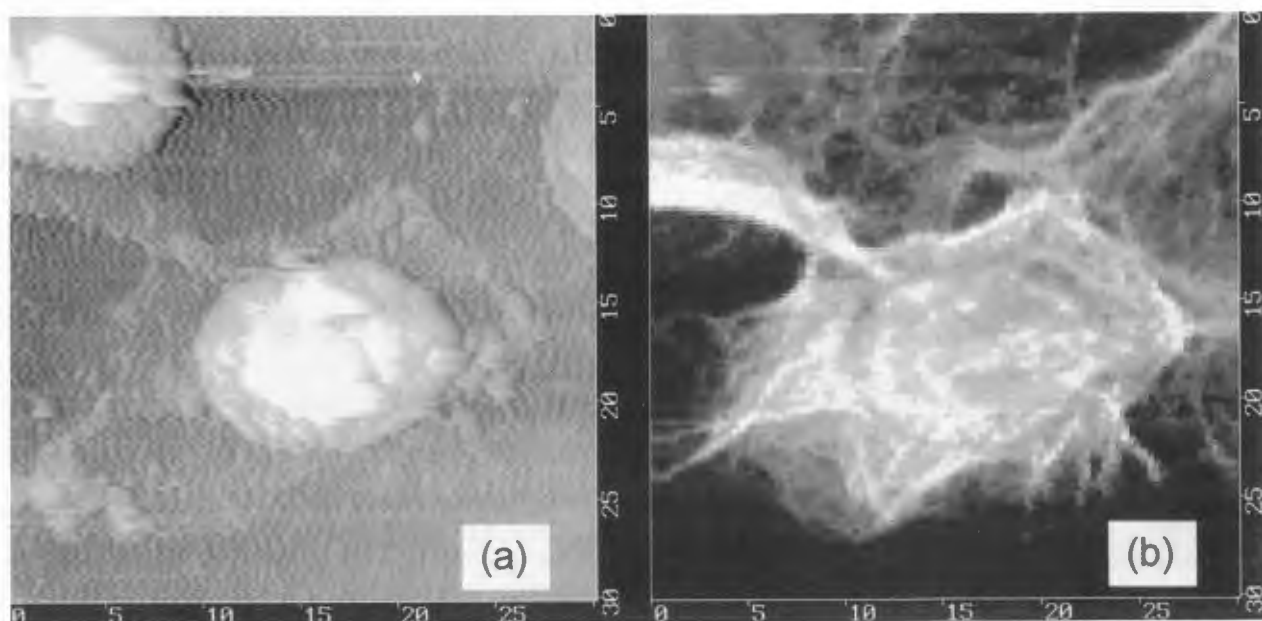


**Figure 8.** Topographic (a) and fluorescence (b) images of cultured cells of human esophageal squamous cell carcinoma (KESC2, C7) in the air in which cell were stained with FITC-labeled phalloidin after treatment with Triton X-100. Scan area is 30  $\mu\text{m}$  by 30  $\mu\text{m}$ .

peak was caused by leaking of the 514.5 nm beam from the polychromatic AO modulator, and easily cut by adding a band pass filter of 488 nm next to the AO modulator. This result shows that SNOM/AFM can obtain spectrograph in a submicron area. This function may be useful in analytical applications in biology and other fields.

Fluorescence and topographic images of cultured cells immunostained with fluorescein isothiocyanate (FITC)-labeled anti-keratin antibody or FITC-labeled phalloidin were obtained in air and water. Figures 8a and 8b show topographic and fluorescence images of cultured cells of human esophageal squamous cell carcinoma (KESC2, C7 subclone) in the air. The cells cultured on collagen-coated cover glass were treated with 1% Triton X-100, stained with FITC-labeled phalloidin and air dried. The topographic image is deteriorated in quality compared with that by normal dynamic mode AFM [14], but it clearly shows the shape of the cell nuclei. On the other hand, the fluorescence image shows actin filaments patterns with high resolution.

Figure 9 shows topographic and fluorescence images of the cultured cells (KESC2, C7) which were immunostained with FITC-labeled anti-keratin antibody after treatment of 1% Triton X-100, and observed by SNOM/AFM in aqueous solution. The fluorescence image shows the precise arrangement of keratin filaments. The topography apparently shows structures corresponding to

keratin filaments as well as round cell nuclei.

The optical images in Figures 8 and 9 recorded 128 lines and 85 pixels per line for a scan of approximately 15 minutes. The images were not displayed to demonstrate optical resolution but to show a possibility of fluorescence imaging in liquid. The appearance resolution from images strongly depends on the sample itself.

The difference of fluorescence images in Figures 8 and 9 is caused because actin filament is a straight structure and keratin filament is a curled structure. Topographic images in Figure 9 show more natural structure than the image in Figure 8, which is a dried up structure. It is better to image the living or nearly living state to obtain the real structure. Therefore, observation of cultured cells is desirable to perform in liquid.

The importance of SNOM/AFM for simultaneous imaging of topography and fluorescence image should be noticed. It enables us to compare topography and fluorescence image. The interest of the cellular specimens is in the display of filament structure, as well as in the distribution of actin and keratin molecules in the cells.

Thus, SNOM/AFM introduces a new method for the study of cellular structures at high resolution unobtainable by conventional optical microscopy. This technique may reveal cell characteristics which are undetected by optical or electron microscopy. In addition, this study suggests that the SNOM/AFM system is widely applicable to specimens in water and other fluid media.



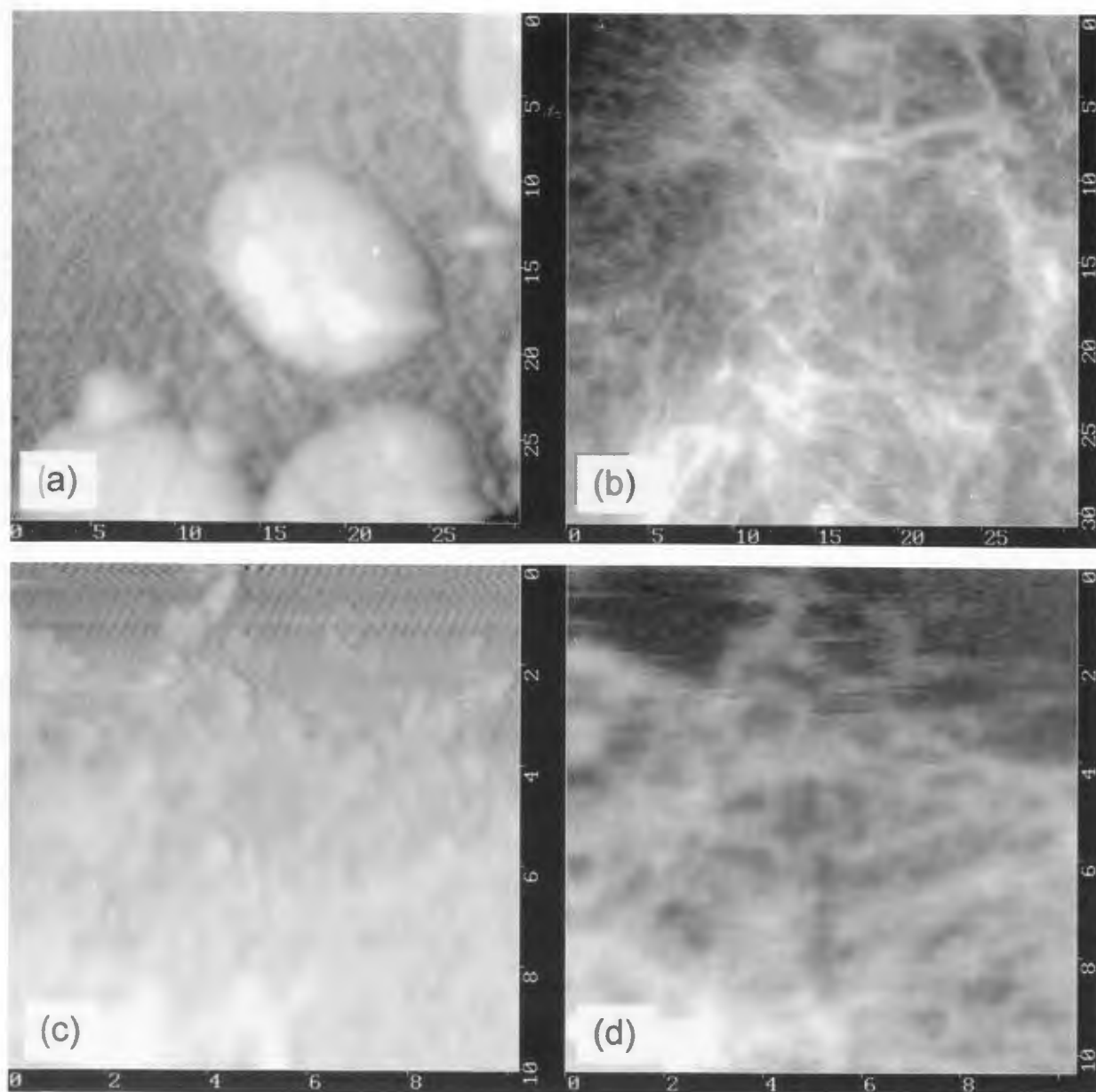


**Figure 9.** Topographic (a and c) and fluorescence (b and d) images of cultured cells of human esophageal squamous cell carcinoma (KESC2, C7) in an aqueous solution, in which cells were stained with FITC-labeled anti-keratin antibody after treatment with Triton X-100. Scan areas are 30  $\mu\text{m}$  by 30  $\mu\text{m}$  (a and b) and 10  $\mu\text{m}$  by 10  $\mu\text{m}$  (c and d).

#### References

- [1] Betzig E, Trautman JK (1992) Near-field optics: Microscopy, spectroscopy, and surface modification beyond the diffraction limit. *Science* **257**: 189-195.
- [2] Chiba N, Muramatsu H, Ataka T, Fujihira M, (1995) Observation of topography and optical image of optical fiber end by atomic force mode scanning near-field optical microscope. *Jpn J Appl Phys* **34**: 321-324.
- [3] Chiba N, Muramatsu H, Nakajima K, Homma K, Ataka T, Fujihira M (1995) Resolution of an optical image of a scanning near-field optical/atomic force microscope as a function of sample-probe distance during synchronized irradiation. *Thin Solid Films* **273**: 331-334.
- [4] Dreier M, Anselmetti D, Richmond T, Dammer

U, Güntherodt HJ (1994) Dynamic force microscopy in liquids. *J Appl Phys* **76**: 5095-5097.

[5] Dürig UT, Pohl DW, Rohner F (1986) Near-field optical-scanning microscopy. *J Appl Phys* **59**: 3318-3327.

[6] Hansma PK, Cleveland JP, Radmacher M, Walters DA, Hillner PE, Bezanilla M, Fritz M, Vie D, Hansma HG (1994) Tapping mode atomic force microscopy in liquids. *Appl Phys Lett* **64**: 1738-1740.

[7] Heinzelman H, Pohl DW (1994) Scanning near-field optical microscopy. *Appl Phys A* **59**: 89-101.

[8] Karrai K, Grober RD (1995) Piezoelectric tip-sample distance control for near field optical microscopes. *Appl Phys Lett* **66**: 1842-1844.

[9] Muramatsu H, Chiba N, Ataka T, Monobe H, Fujihira M (1995) Scanning near-field optic/atomic force microscopy. Proceedings of second conference on near-field optics, Raleigh, NC, 20-22 October 1993. *Ultramicroscopy* **57**: 141-146.

[10] Muramatsu H, Chiba N, Homma K, Nakajima K, Ataka T, Ohta S, Kusumi A, Fujihira M (1995) Near-field optical microscopy in liquids. *Appl Phys Lett* **66**: 3245-3247.

[11] Muramatsu H, Chiba N, Umemoto T, Homma K, Nakajima K, Ataka T, Ohta S, Kusumi A, Fujihira M (1995) Development of near-field optic/atomic force microscopy for biological materials in aqueous solutions. *Ultramicroscopy* **61**: 265-269.

[12] Putman CAJ, Van der Werf KO, De Grooth B G, Van Hulst NF, Greve J (1994) Tapping mode atomic force microscopy in liquids. *Appl Phys Lett* **64**: 2454-2456.

[13] Shalom S, Lieberman K, Lewis A (1992) A micropipette force probe suitable for near-field scanning optical microscopy. *Rev Sci Instr* **63**: 4061-4065.

[14] Ushiki Y, Shigeno M, Abe K (1994) Atomic force microscopy of embedment-free sections of cells and tissues. *Arch Histol Cytol* **57**: 427-432.

[15] van Hulst NF, Moers MHP, Noordman OFJ, Tack RG, Segerink FB, Bölger B (1993) Near-field optical microscope using a silicon-nitride probe. *Appl Phys Lett* **62**: 461-463.

**Editor's Note:** All of the reviewer's concerns were appropriately addressed by text changes, hence there is no Discussion with Reviewers.